International Journal of Bridge Engineering (IJBE), Special Issue 2016, pp. 97-115

INFLUENCE OF CABLE FAILURE MECHANISMS ON THE DYNAMIC BEHAVIOR OF CABLE STAYED BRIDGES

Domenico Bruno, Fabrizio Greco and Paolo Lonetti*

University of Calabria, Dept. of Civil Engineering, Italy
e-mail: d.bruno@unical.it, f.greco@unical.it lonetti@unical.it, lonetti@unical.it

ABSTRACT: An analysis on the effects produced by failure mechanisms in the cable system is proposed to investigate the behavior of cable-stayed bridges. In particular, the present paper aims to verify the influence on the bridge behavior of accidental breakages produced in the cable system elements also in light of existing design guidelines available from the literature. In the present paper, the numerical model is based on a refined description of the bridge, which involves bridge constituents and external loads. In particular, a geometric nonlinear formulation in which the effects of local vibrations in the stays and large displacements in girder and pylons are taken into account. Moreover, damage effects are simulated by using an accurate description of the release effects produced by the cable-breakage processes. The results denote that several parameters associated with cable-breakage processes, such as the breakage duration, time-transient curve and external load description, are found to influence the dynamic performance of the bridge.

KEYWORDS: Cable-stayed bridges; cable-cutting; design guidelines, damage mechanics.

1 INTRODUCTION

Stays or hangers are typically employed to create an enhanced structural system able to transfer internal forces between bridge components with lightness, efficiency and reduced costs. In particular, in cable-stayed bridges, the presence of the cables allows the transferring of the forces from the girder to the pylon and facilitates the construction by the cantilever method. However, the cables are typically exposed to several damage mechanisms, such as fatigue processes, corrosion or abrasion, which may cause of a reduction of the cross-section and the strength of the element. As a consequence, the cables are much exposed to failure mechanisms, whose breakage may produce force redistributions and unexpected load configurations. Currently, design guidelines are proposed mainly for cable-stayed bridges, in which specific load combinations concerning dead, live and impact loads are considered. As a matter of fact, PTI

*Corresponding Author

[1] and SETRA [2] propose an equivalent static analysis in which a Dynamic Amplification Factor (DAF) is suggested to reproduce the accidental situations. In particular, in order to identify the amplification effects provided by the failure mechanism in the cable system, existing codes recommend to amplify the results obtained in the framework of static analyses by using fictitious amplification factors suggested in the range between 1.5 and 2.0.

Moreover, the stress distribution arising from such a loading scheme is combined with the effects of other existing loading schemes by means of proper factored loading combinations. Alternatively, the design codes leave the designer to develop a dynamic analysis, by computing the cable release effects by analyzing the time-history of the structural response of each design variables. Such approach is quite difficult to be developed since the complete evaluation of the worst damage scenarios, requires to develop long time-history data, since it is necessary to examine the influence of damage mechanisms at any locations of the bridge as well as the possibility that single and multiple cables can be affected by failure mechanisms simultaneously.

In the literature, the consistency of the design guidelines is verified only by very few comprehensive investigations and, mainly for cable-stayed or suspension bridges schemes. In particular, recent papers have demonstrated that design prescriptions become unsafe in many cases, leading to dynamic amplification factors larger than those suggested by existing recommendations [3, 4]. In particular, some parametric studies have been developed for bridge typologies subjected to accidental cable failure by using a numerical approach based on classical standard linear dynamic framework [3, 5, 6]. Such analyses, referred to small or medium span bridges, denote that the results obtained by using such code prescriptions are affected by high underestimations in the prediction of typical design bridge variables related to the girder and pylons. The analyses referred to above do not include in the investigations the effects produced from the dynamic interaction between moving loads and bridge vibrations or from an accurate description of the cable failure. Actually, many works available from the literature are devoted to investigate dynamic bridge behavior for undamaged structures, which show how the influence of external mass and the presence of inertial forces produced by nonstandard accelerations function may involve large dynamic amplifications in both kinematic or stress variables [7, 8].

In addition, the analysis of cable failure mechanisms produced by loss of stiffness due to cable degradation or due to accidental failure is rarely analyzed. Typically, many papers investigate the cable failure of a single element with localized or distributed independent mechanisms [9, 10]. In the framework of cable supported bridges the analysis of the bridge under damage mechanism should involve details concerning the time dependent characteristics of the failure mode or the coupling behavior between damaged and undamaged elements of the cable system. In the present paper, the analyses developed in

[11, 12] for cable-stayed, bridges will be discussed introducing more details.

The aim of the paper is to propose a parametric study to investigate the influence on the bridge behavior of the dynamic excitation produced by damage mechanisms in the cable system and by the transit of moving loads. The outline of the paper is as follows: Section 2 presents the general formulation of the cable and the girder elements and the damage description of the cable model; the numerical implementation is reported in Section 3; parametric studies in terms of bridge and moving loads characteristics and failure mode typology in the cable system are reported in Section 4.

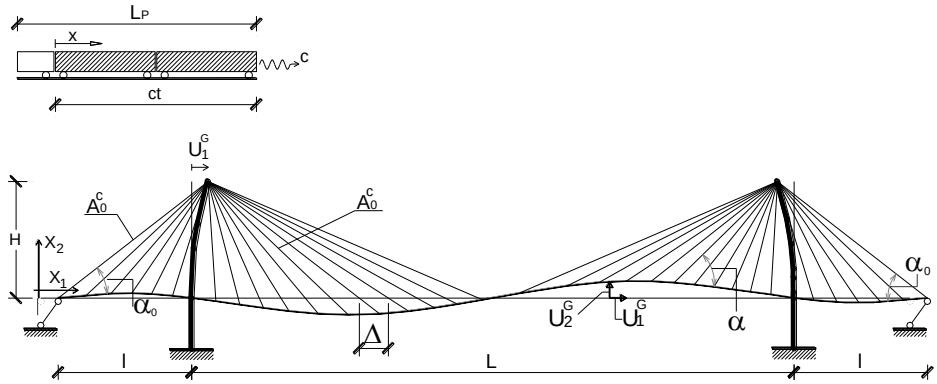

Figure 1. Cable stayed bridge configuration and kinematics

2 THEORETICAL FORMULATION AND GOVERNING EQUATIONS

In this section the governing equations for the bridge constituents for the cable stayed as well as the main assumptions concerning the kinematic modeling are discussed. In particular, the structural model concerning cable-stayed configuration is consistent with a fan-shaped and a self-anchored cable-stayed bridge scheme (Fig.1). The stays are hinged, at both ends, to the girder and pylons. The bridge formulation is based on a one-dimensional truss approach to simulate the cable system behavior and a beam modeling to analyze girder and pylon deformations. The cable elements are defined by means of a nonlinear geometric truss formulation, in which both local and global vibrations are taken into account by using a proper number of mesh elements along the cable development [11].

2.1 Cable formulation and damage phenomena

The constitutive laws of the cables are defined by the second Piola-Kirchhoff stress $\left(S_1^C\right)$ and Green-Lagrange strain $\left(E_1^C\right)$ as follows:

$$S_1^C\left(\underset{\sim}{X},t\right)=S_0^C+C^C\left[1-\xi_i\left(\underset{\sim}{X},t\right)\right]E_1^C\left(\underset{\sim}{X},t\right) \tag{1}$$

with

$$E_1^C\left(\underset{\sim}{X},t\right)=U_{1,X_1}^C\left(\underset{\sim}{X},t\right)+\frac{1}{2}\left[U_{1,X_1}^2\left(\underset{\sim}{X},t\right)+U_{2,X_1}^2\left(\underset{\sim}{X},t\right)+U_{3,X_1}^3\left(\underset{\sim}{X},t\right)\right]^C \tag{2}$$

where C^C is the elastic modulus and S_0^C is the stress referred to the initial configuration.

Moreover, ξ_i, with *i=st,dn* refers to the static or dynamic definition of the damage variable, whose description is consistent to the Continuum Damage mechanics (CDM) theory [13, 14]. In particular, the presence of damage mechanisms in the cable system, involved by degradation phenomena, is supposed to produce a reduction of the cross-section area, on the basis of the following expression:

$$\xi_i\left(\mathrm{s},t\right)=\frac{C^CA^C\left(s,t\right)-\overline{C^CA^C}\ \left(s,t\right)}{C^CA^C\left(s,t\right)}\quad with\quad \xi_i\in\left[0,1\right] \tag{3}$$

where s is the curvilinear coordinate used to describe the arc-length of the cable, C^CA^C and $\overline{C^CA^C}$ are the actual and residual stiffnesses of the cable element, respectively.

Moreover, according to experimental evidence [15] on the failure mechanisms of cable elements, the dynamic evolution of the damage variable is defined by means of a one dimensional formulation based on a Kachanov's law on the basis of the following expression:

$$\xi_d\left(s,t\right)=\left[1-\frac{\left(t-t_0\right)\left[1-\left(1-\xi_s\right)^{m+1}\right]}{t_f}\right]^{1/m+1} \tag{4}$$

where *m* is asymptotic parameter of the damage evolution and $\left(t_0,t_f\right)$ are the initial and final times describing the failure mechanism.

A synoptic representation of the damage law is reported in Fig. 2. It is worth noting that Eq.(4) corresponds to a damage law, whose degradation function is able to include different evolutions of the damage curves depending from the exponential parameter *m*.

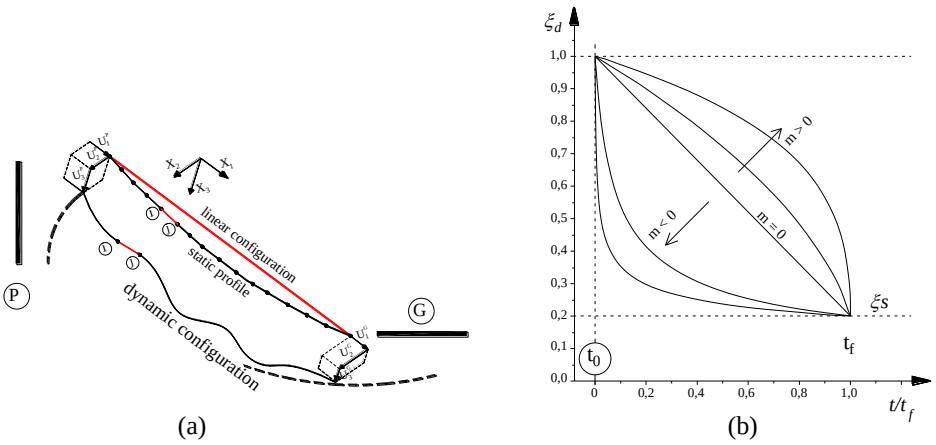

Figure 2. Damage configuration of the cable (a) and dynamic degradation function (b)

2.2 Moving loads

The external loads are consistent with uniformly distributed vertical moving forces and masses, travelling on the girder profile at constant speed (c), whereas frictional forces and roughness effects arising from the girder profile are supposed to be negligible. The analytic description of the moving mass function λ , acting on the girder profile, is defined as:

$$\lambda = \lambda\left(X_1, t\right) = \lambda_{ML}\,\overline{H}\left(X_1 + L_p - ct\right)\overline{H}\left(ct - X_1\right) \tag{5}$$

where $\overline{H}\left(\cdot\right)$ is the Heaviside step function, L_p is the length of the moving loads and λ_{ML} is the mass linear density of the moving system and X_1 is the abscissa coinciding to the geometric axis direction of the girder. Moreover, the expression of the moving loads, for a fixed inertial reference frame $\left(0, \underset{\sim}{n}_1, \underset{\sim}{n}_2, \underset{\sim}{n}_3\right)$ is defined by the weight and the inertial forces produced by the inertial characteristics and the unsteady mass distribution of the moving loads along the girder, as follows [16]:

$$p_{X_i} = \lambda g\ \underset{\sim}{n}_i \times \underset{\sim}{n}_3 + \frac{d}{dt}\left[\lambda \frac{d\overline{U}_i^m}{dt}\right] = \lambda g\ \underset{\sim}{n}_i \times \underset{\sim}{n}_3 + \frac{d\lambda}{dt}\frac{d\overline{U}_i^m}{dt} + \lambda \frac{d^2\overline{U}_i^m}{dt^2}, \tag{6}$$

where $\overline{\underset{\sim}{U}}^m$ is the moving load kinematic which can be expressed as a function of the displacement and rotation fields of the centroid axis of the girder. Since the external forces, defined by Eq.s (5)-(6), are described in terms of a moving coordinate, the time dependent description introduces the following expressions for the velocity and the acceleration functions [8]:

$$\begin{aligned}
\frac{d\,\bar{U}_i^m}{dt} &= \frac{\partial \bar{U}_i^m}{\partial t} + \frac{\partial \bar{U}_i^m}{\partial t} c, \\
\frac{d^2 \bar{U}_i^m}{dt^2} &= \frac{\partial^2 \bar{U}_i^m}{\partial t^2} + 2c \frac{\partial^2 \bar{U}_i^m}{\partial t \partial X_1} + c^2 \frac{\partial^2 \bar{U}_i^m}{\partial X_1^{\,2}},
\end{aligned} \tag{7}$$

where the three terms at the r.h.s. of Eq.(7).2 correspond to the standard, centripetal and Coriolis acceleration functions.

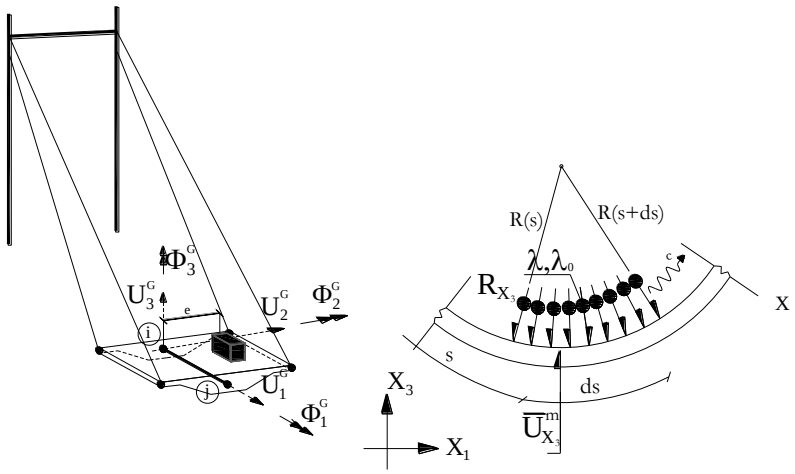

Figure 3. Moving loads description and evaluation of the external forces

Finally, on the basis of Eq.s (6)-(7), assuming that the mass does not separate from the beam during its horizontal and vertical vibrations, the external load functions are defined by the following relationships:

$$\begin{aligned}
p_{X_1} &= \frac{d\lambda}{dt}\left[\left(\frac{\partial U_1^G}{\partial t} - e\frac{\partial^2 U_2^G}{\partial t \partial X_1}\right)\right] + \lambda \frac{\partial^2 U_1^G}{\partial t^2} - \lambda \cdot e \frac{\partial^3 U_3^G}{\partial t^2 \partial X_1}, \\
p_{X_2} &= \frac{d\lambda}{dt}\frac{\partial U_2^G}{\partial t} + \lambda \frac{\partial^2 U_2^G}{\partial t^2}, \\
p_{X_3} &= \lambda g + \frac{d\lambda}{dt}\left[\left(\frac{\partial U_3^G}{\partial t} + e\frac{\partial \Psi_1^G}{\partial t}\right) + c\left(\frac{\partial U_3^G}{\partial X_1} + e\frac{\partial \Psi_1^G}{\partial X_1}\right)\right] + \\
&+ \lambda\left[\frac{\partial^2 U_3^G}{\partial t^2} + 2c\frac{\partial^2 U_3^G}{\partial t \partial X_1} + c\frac{\partial^2 U_3^G}{\partial X_1^{\,2}}\right] + \lambda \cdot e\left[\frac{\partial^2 \Psi_1^G}{\partial t^2} + 2c\frac{\partial^2 \Psi_1^G}{\partial t \partial X_1} + c\frac{\partial^2 \Psi_1^G}{\partial X_1^{\,2}}\right].
\end{aligned} \tag{8}$$

where (X_1, X_2, X_3) are the coordinate system described in Fig.3, (U_1^G, U_2^G, U_3^G) and $(\Phi_1^G, \Phi_2^G, \Phi_3^G)$ are the displacement and rotation fields of the

centroid axis of the girder with respect to the global reference system respectively.

2.3 Girder and pylon formulation

The formulation of the pylons and the girder is consistent with a geometric nonlinear model based on Euler-Bernoulli theory, in which large displacements are considered by using Green–Lagrange strain measure. The constitutive relationships are defined on the basis of moderately large rotations in which only the square of the terms representing the rotations of the transverse normal line in the beam is considered.

Moreover, the governing equations are expressed as a function of the X_1 variable, which coincides with the longitudinal ($X=X_1$). Therefore, starting from the status concerning the initial configuration of the bridge the following relationships between generalized strain and stress variables are adopted for the Girder (G) description:

$$\begin{aligned}
&N_1^G = N_1^{0(G)} + EA^G \varepsilon_1^G = N_1^{0(G)} + E^G A^G \left\{ U_{1,X_1}^G + \frac{1}{2}\left[U_{1,X_1}^{2G} + U_{2,X_1}^{2G} + U_{3,X_1}^{2G} \right] \right\} \\
&M_2^G = M_2^{0(G)} + EI_2^G \chi_2^G = M_2^{0(G)} + E^G I_2^G \Phi_{2,X_1}^G = M_2^{0(G)} - EI_2^G U_{3,X_1 X_1}^G , \\
&M_3^G = M_3^{0(G)} + EI_3^G \chi_3^G = M_3^{0(G)} + E^G I_3^G \Phi_{3,X_1}^G = M_3^{0(G)} + EI_3^G U_{2,X_1 X_1}^G , \\
&M_1^G = GJ_t^G \Theta^G = G^G J_t^G \Phi_{1,X_1}^G ,
\end{aligned} \tag{9}$$

where EA^G and ε_1^G are the axial stiffness and strain, χ_2^G and χ_3^G or $E^G I_2^G$ and $E^G I_3^G$ are the curvatures or the bending stiffnesses with respect to the X_2 and X_3 axes, respectively, Θ^G and $G^G J_t^G$ are the torsional curvature and stiffness, respectively, N_1^G is the axial stress resultant, M_2^G and M_3^G are the bending moments with respect to the X_2 and X_3 axes, respectively, M_1^G and $G^G J_t^G$ are torsional moment and girder stiffness, respectively, and $(\cdot)^0$ represents the superscript concerning the variables associated with the "initial status under dead loads ".

However, the governing equations concerning the pylons are exactly equal to ones reported in Eq.(9) and thus, for the sake of brevity will not reported. It is worth noting that the evaluation of the initial configuration is based on a proper procedure, in which post-tensioning stresses and cross-sections of the cables are designed in such a way that the bridge remains practically in the undeformed configuration under dead loads. More details concerning the procedure utilized in the present paper can be recovered in [17-19]

3 NUMERICAL IMPLEMENTATION

A numerical approach based on the finite element formulation is utilized. In particular, introducing Hermit cubic interpolation functions for the girder and pylon flexures in the X_1X_2 and X_2X_3 deformation planes and Lagrange linear interpolation functions for the cable system variables and the remaining variables of the girder and the pylons the following displacements vector are determined:

$$\begin{aligned} \underset{\sim}{U}^C(\underset{\sim}{r},t) &= \underset{\sim}{N}^C(\underset{\sim}{r})\underset{\sim}{q}^C(t), \\ \underset{\sim}{U}^G(\underset{\sim}{r},t) &= \underset{\sim}{N}^G\underset{\sim}{q}^G(t), \\ \underset{\sim}{U}^P(\underset{\sim}{r},t) &= \underset{\sim}{N}^P\underset{\sim}{q}^P(t), \end{aligned} \tag{10}$$

where $\underset{\sim}{q}_C, \underset{\sim}{q}_G$ and $\underset{\sim}{q}_P$ are the vectors collecting the nodal degrees of freedom of the cable, girder and pylon respectively, $\underset{\sim}{N}_C, \underset{\sim}{N}_G$ and $\underset{\sim}{N}_P$ are the matrixes containing the displacement interpolation function for Cable element (C), Girder (G)and Pylons (P) and $\underset{\sim}{r}$ is the local coordinate vector of the *i*-th finite element. Finally, taking into account the balance of secondary variables at the interelement boundaries, the resulting equations of the finite element model are:

$$\underset{\sim}{M}\ddot{\underset{\sim}{Q}} + \underset{\sim}{C}\dot{\underset{\sim}{Q}} + \underset{\sim}{K}\underset{\sim}{Q} = \underset{\sim}{P} \tag{11}$$

where $\underset{\sim}{Q}$ with $\underset{\sim}{Q} = \underset{\sim}{U}_B \cup \underset{\sim}{U}_G \cup \underset{\sim}{U}_P$ is the generalized coordinate vector containing the kinematic variables associated with the girder, the pylons and the cable system, $\underset{\sim}{M}$, $\underset{\sim}{C}$ and $\underset{\sim}{K}$ are the global mass, stiffness and damping matrixes and $\underset{\sim}{P}$ is the loading vector, containing also nonstandard terms arising from moving load description. Since the structural behavior of each element depends on the deformation state of the members, the governing equations defined by Eq.(11) will change continuously as the structure deforms.

Moreover, the external loads owing to the presence of its own moving mass determine a time dependent mass distribution function on the girder profile. Consequently, the discrete equations are affected by nonlinearities in the stiffness matrix and time dependence in the mass matrix. The governing equations are solved numerically, using a user customized finite element program, i.e. COMSOL Multiphysics TM version 4.1 [20]. The algebraic equations are solved by a direct integration method, which is based on an implicit time integration scheme. In particular, an implicit temporal discretization of order two using a Backward Differentiation Formula (BDF-2) with an adaptive time step is utilized. Moreover, a Newton-Raphson scheme in the time step increment based on the secant formulation is utilized for the nonlinearities involved in the governing equations. In order to guarantee accuracy in the predicted results, particular attention is devoted to the choice of

the time integration step, which, assuming small vibrations about the non-linear equilibrium configuration under dead loads, can be defined as a function of the periods of those vibration mode shapes having a relevant participation on the response. However, in the case of moving load excitation, the dynamic solution strongly depends from the speed of the moving system, since different vibration frequencies are activated for low or large transit speeds [21]. In the present analyses, the initial integration time step, which is automatically reduced due to the time adaptation procedure, is assumed as at least 1/1000 of the observation period defined as the time necessary for the moving train to cross the bridge. This value turns out to be always lower than 1/100 of the 50th natural period of the bridge structure, the first natural period being the largest one.

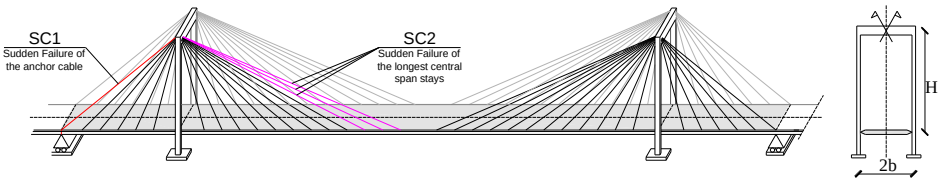

Figure 4. Damage scenarios of the cable-systems

4 RESULTS

Numerical results are reported to investigate the influence of damage mechanisms involved in the cable system for both cable-stayed and tied arch bridges. The investigation is developed on a long span bridge typology, with main span length (L) equal to 1000 m. The deck is made of steel with aerodynamic cross section, *4* m depth and *20* m wide; the vertical moment of inertia $\left(\mathrm{I}_2^G\right)$, the transverse moment of inertia $\left(\mathrm{I}_3^G\right)$, the cross section area $\left(\mathrm{A}^G\right)$ the torsional constant $\left(\mathrm{J}^G\right)$ and the modulus of elasticity of steel E^G for the bridge deck are *3.41* m^4, *31* m^4, 2.1 m^2, 15 m^4, 2.1×10^8 kN/m^2, respectively. The towers are formed by *H*-shaped steel elements, whose elements present vertical moment of inertial $\left(\mathrm{I}_2^P\right)$, transverse moment of inertia $\left(\mathrm{I}_3^P\right)$, cross section area $\left(\mathrm{A}^P\right)$, torsional constant $\left(\mathrm{J}^P\right)$ and modulus of elasticity $\left(C^G\right)$ equal to 20.57 m^4, 9.78 m^4, 1.97 m^2, 21.13 m^4, 2.1×10^8 kN/m^2, respectively. Moreover, the limit elastic bending moment $\left(M_{20}^P\right)$ and the normal stress resultant $\left(N_{10}^P\right)$ are equal to 1.85×10^9 N$\cdot$m and 6.84×10^8 N. The stays and the hangers present a distance equal to 20 m and present allowable stress ($\mathrm{S_a}$) equal to 7.2×10^8 Pa. Finally, dead loading of the girder including also permanent loads are equal to 3.0×10^5 N/m, whereas the ratio between live and dead loads

is equal to 0.5. The initial configuration is defined according to the iterative procedure described in Section 4. The analyses are developed with the purpose of investigating the effect of the cable failure on the stress distribution in the bridge components and the corresponding dynamic influence produced by the cable release mechanisms. To this aim two different damage scenarios, represented in Fig. 4, are considered, in which the damage mechanisms are assumed to affect the cable stayed system, at the anchor stay (SC1) or at the stays in the central span (SC2). In particular, the damage scenarios SC1 and SC2 consider the failure of the anchor stay and the longest three stays of the main span. In order to quantify, numerically, the vulnerability of a bridge component, a dimensionless parameter, ranging from 0 to 1, is defined as the reduction ratio of the load multiplier from the undamaged to the damaged configurations:

$$V_I = \frac{\Gamma_{UD} - \Gamma_D}{\Gamma_{UD}} \tag{12}$$

where Γ_{UD} and Γ_D are the loading carrying capacities with respect to the allowable quantity before and after an unpredictable damage mechanism. Moreover, dynamic amplification factors (DAFs), for the generic variable Γ under investigation related to Damaged (D) or UnDamaged (UD) structural configuration, are defined by the following relationships:

$$\begin{aligned}
\Phi_{\Gamma}^{D} &= \frac{\max\left(\Gamma^{D}, t = 0..T\right)}{\Gamma_{ST}^{D}}, \\
\Phi_{\Gamma}^{UD} &= \frac{\max\left(\Gamma^{UD}, t = 0..T\right)}{\Gamma_{ST}^{UD}}, \\
\Phi_{\Gamma}^{D-UD} &= \frac{\max\left(\Gamma^{D}, t = 0..T\right)}{\Gamma_{ST}^{UD}},
\end{aligned} \tag{13}$$

where T is the observation period and the subscript $(\bullet)_{ST}$ refers to the value of the variable determined in a static analysis. Moreover, an additional description of the DAFs is reported in the results is defined according to the relationship recommended by the PTI codes [1]:

$$\Phi_{\Gamma}^{PTI} = \frac{\max\left(\Gamma^{D}, t = 0..T\right) - \Gamma_{ST}^{UD}}{\Gamma_{ST}^{D} - \Gamma_{ST}^{UD}}, \tag{14}$$

At first, the effects of the cable failure are evaluated on the loading scheme, involving dead loads only. The main aim of such results is to investigate the effects of the cable release arising from an accidental cable failure and to quantify the corresponding dynamic amplification factors, also in the light of

the actual recommendations provided by existing codes on cable supported bridges [3,4]. Results in terms of vertical displacements and torsional rotations of the girder, namely U_3^G / L and $\Psi_1^G B / L$. With reference to Fig. 5, comparisons, concerning SC1 and SC2 damage scenarios, denote that the failure in the anchor cable or the stay elements affects the girder deformation, mainly in the cable-stayed bridge scheme, producing notable vertical displacements and torsional rotations. Such values are larger than the corresponding ones commonly recommended for the serviceability limit state by codes on cable-supported bridges. Moreover, the failure of the anchor stay seems to produce greater vulnerability than the damage mechanisms SC2, since larger deformations are observed. Comparisons between static and dynamic damage modes denote that the dynamic characteristics of the cable release effect influence mainly vertical displacements for both SC1 and SC2 damage scenarios, whose maximum DAFs are equal to 1.9 for both bridge schemes. Results concerning girder torsional rotations denote that the DAFs are much lower than those observed for vertical displacements. In particular, the SC1 damage scenario produces a DAF equal to 1.31, whereas for the SC2 damage scenario the dynamic amplification effects are practically negligible and thus the corresponding DAF is close to the unity.

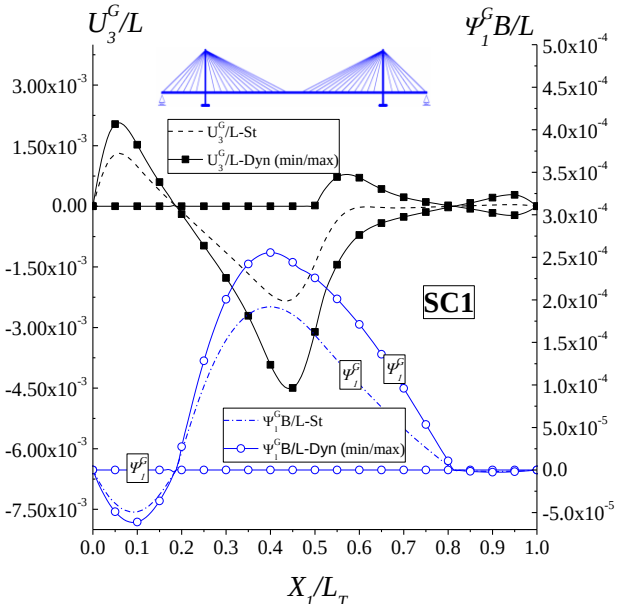

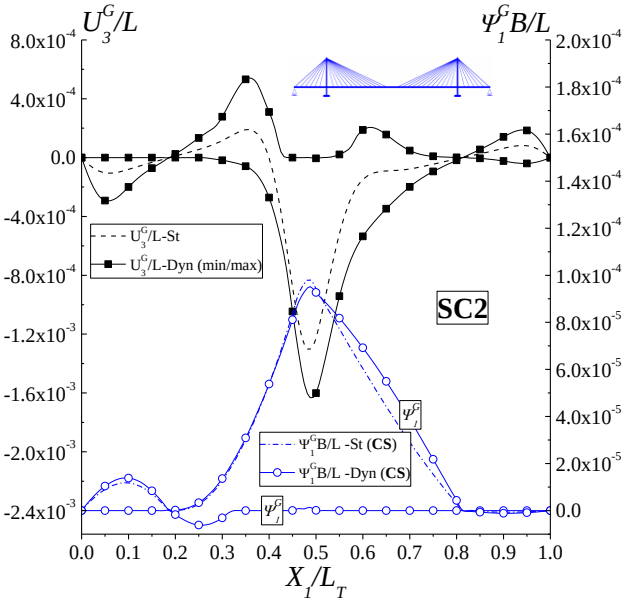

Figure 5. Girder deformability under the action of dead loads (DL) for the damage scenarios SC1-SC2

The analyses are extended to the loading combinations involving the presence of live loads (LL), taking into account, in those cases in which the calculation is developed in dynamics, the inertial effects produced by moving loads.

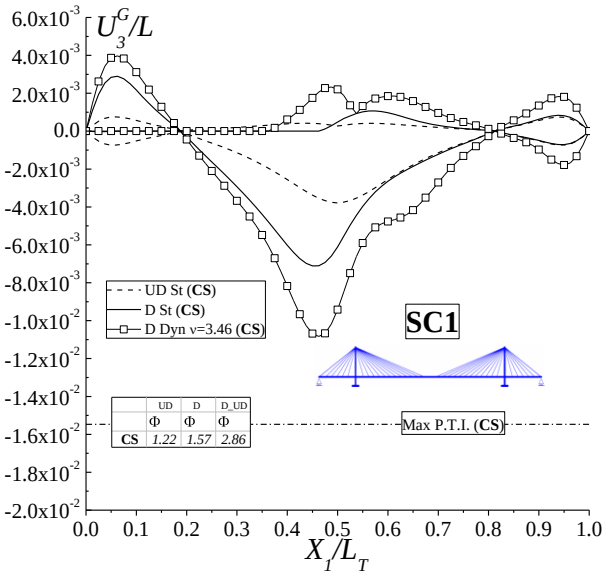

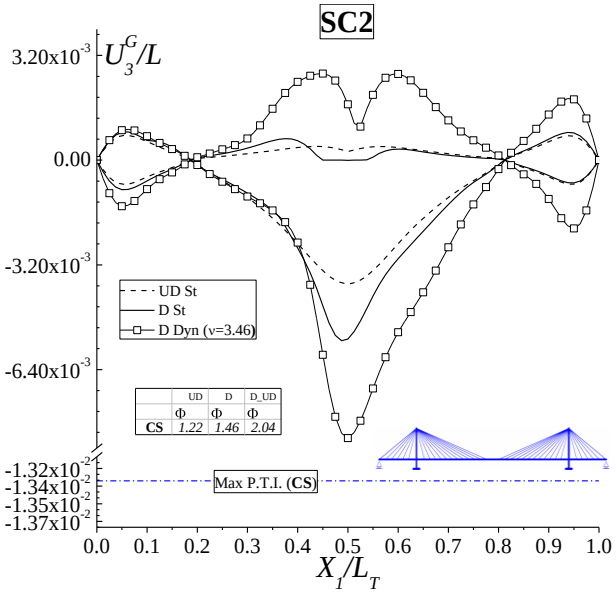

Figure 6. Girder deformability under the action of dead loads (DL) for the damage scenarios SC1-SC2

In particular, the vulnerability behavior of the bridge structures is analyzed for all the damage scenarios in terms of girder displacements. The main purpose of the results is to provide an easy evaluation on the bridge capacity to redistribute the overall stresses produced by the cable release. The analyses collect results arising from static cases in the damaged (D) and undamaged (UD) configurations, taking into account the dynamic effects produced by moving loads at high speed ranges, i.e. $\upsilon = c\left(\frac{\mu_G}{gH}\right)^{1/2} = 3.46$. The results, reported in Figs. 6 for the investigated scenarios, show how both bridge systems are affected by the presence of the damage mechanisms, since the prediction of vertical displacements is strongly modified from the UD cases. Moreover, the DAFs reported in the same figures, give a numerical evaluation on how the deformability of the bridge, affected by damage mechanisms, is amplified with respect to the undamaged configuration.

Additional results are presented to analyze the influence of the damage mechanisms on the stress distribution in the cable system. For the assumed damage scenarios, the envelope of the stress distribution normalized on the allowable stress is analyzed. In particular, in Fig. 7 results concerning SC1 damage scenario are reported, which show how cable-stayed system is affected by stresses amplifications, mainly in the region close to the cable failure. In the cable stress distribution the PTI prediction overestimates the actual DAFs

predicted by the proposed modeling. Finally, the vulnerability index, defined according to Eq.(12), clearly show how the worst damage value is observed in proximity of the anchor cable.

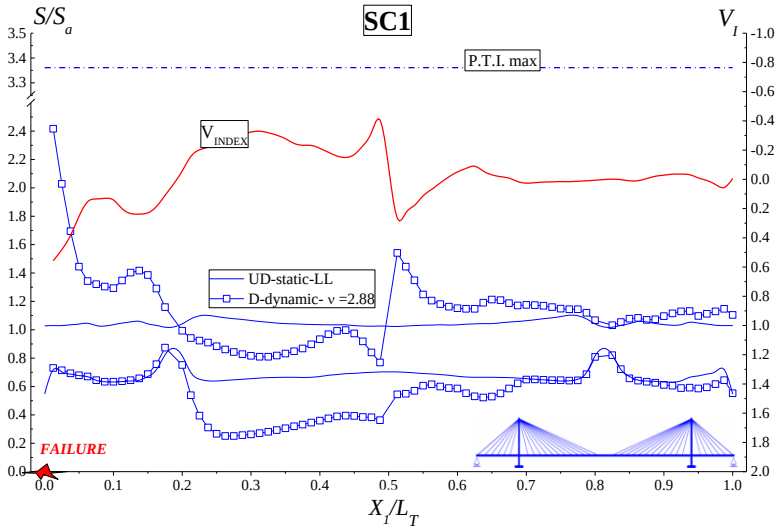

Figure 7. Cable-stayed bridge: envelope stress distribution in the cable systems under the action of live loads (LL) and vulnerability behavior for the damage scenario SC1

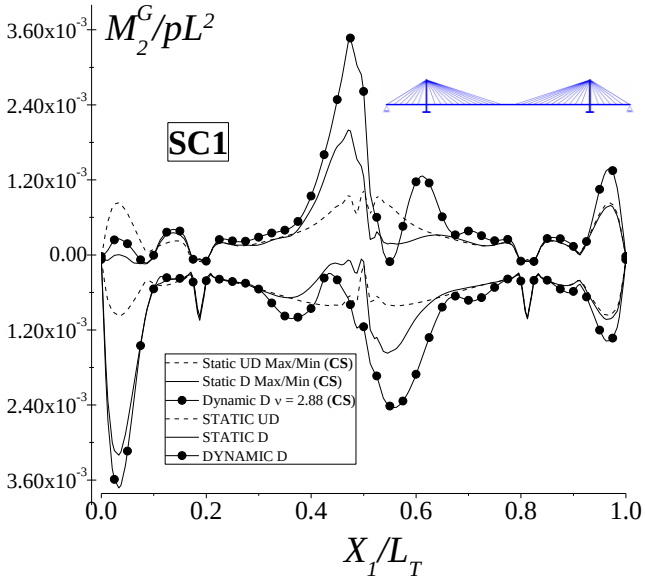

Figure 8. Cable-stayed bridge: envelope stress distribution in the cable systems under the action of live loads (LL) and vulnerability behavior for the damage scenario SC1

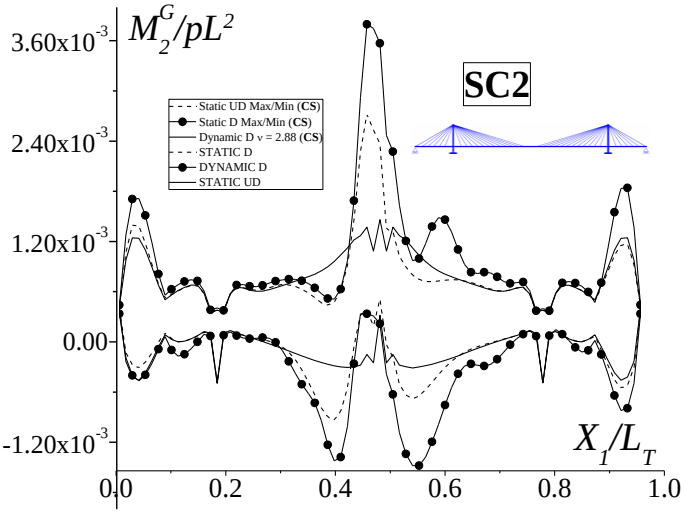

Figure 9. Cable-stayed bridge: envelope stress distribution in the cable systems under the action of live loads (LL) and vulnerability behavior for the damage scenario SC1

Results in terms of bending moments of pylons and girder are proposed, by means of comparisons between damaged, undamaged bridge schemes for the SC1 and SC2 damage scenarios.

In particular, in Fig.8-9 the envelope of bending moments for the cases of dynamic damaged, static damaged and static undamaged configurations are analyzed. The behavior of the bridge is analyzed to investigate the relationship between dynamic amplification factors (DAFs) and the normalized speed parameter of the moving system, i.e. $\Theta = c\left(\frac{\mu_G \sigma_g}{E^G g H}\right)^{1/2}$ as a function of the tower topology and the moving mass schematization. Moreover, the amplification effects produced by the damage mechanisms are quantified on the basis of different damage descriptions defined by Eqs.(13) and the corresponding results are reported in Table 1, in which bending moments at several cross-sections at base of the pylons are investigated. The results denote that the cable stayed bridges are affected by important amplification effects, which are much larger than the allowable values defined by existing codes on ALS. Large amplifications are observed in proximity of the midspan cross section, since, in such region, a reduction of the support condition produced by the anchor cable is typically observed in undamaged cable-stayed bridge configuration.

Table 1. Dynamic amplification effects for the damage scenario SC1-SC2 in terms of bending moments at the lowest cross-sections of the pylons

SC1						
Base (X_1,X_2)	M^{UD}_{ST}/pL^2 ($x10^{-3}$)	M^{D}_{St}/pL^2 ($x10^{-3}$)	M^{D}_{Dvn}/pL^2 ($x10^{-3}$)	Φ^{UD}	Φ^{D}	Φ^{D-UD}
Left (X_3=-b)	3.236	10.685	12.829	1.24	1.20	3.96
Left (X_3=b)	2.582	3.244	4.896	1.38	1.51	1.90
Right (X_3=-b)	-3.208	-7.516	-8.541	1.56	1.14	2.66
Right (X_3=b)	-2.555	-6.642	-7.750	1.73	1.17	3.03

SC2						
Base (X_1,X_2)	M^{UD}_{ST}/pL^2 ($x10^{-3}$)	M^{D}_{St}/pL^2 ($x10^{-3}$)	M^{D}_{Dvn}/pL^2 ($x10^{-3}$)	Φ^{UD}	Φ^{D}	Φ^{D-UD}
Left (X_3=-b)	3.236	2.555	3.367	1.24	1.32	1.04
Left (X_3=b)	2.582	3.227	4.332	1.38	1.34	1.68
Right (X_3=-b)	-3.208	-3.161	-5.348	1.56	1.69	1.67
Right (X_3=b)	-2.555	-2.463	-4.793	1.73	1.95	1.88

Finally, the dynamic response of the bridge is evaluated by means of comparisons between damaged (D) or undamaged bridge (UD) structures. The results, reported in Fig.s 10, are defined through the relationships between moving system normalized speed and dynamic amplification factors for the midspan vertical displacement and bending moment in the damage scenario SC1. Nevertheless, the DAF evolution curves denote a tendency to increase with the speeds of the moving system. The results show that the DAFs developed for bridge structures affected by a failure mechanisms in the cable system are, typically, larger than those obtained assuming undamaged bridge configurations. Moreover, underestimations in the DAF predictions are observed in those cases, in which the inertial contributions arising from the external moving mass are completely neglected. The analyses presented above in terms of the DAFs Φ_X^{D-UD} for both the damaged and undamaged configurations, point out that bridge structures with A or H shaped typologies undergoing damage are characterized by large dynamic amplifications with respect to the undamaged case.

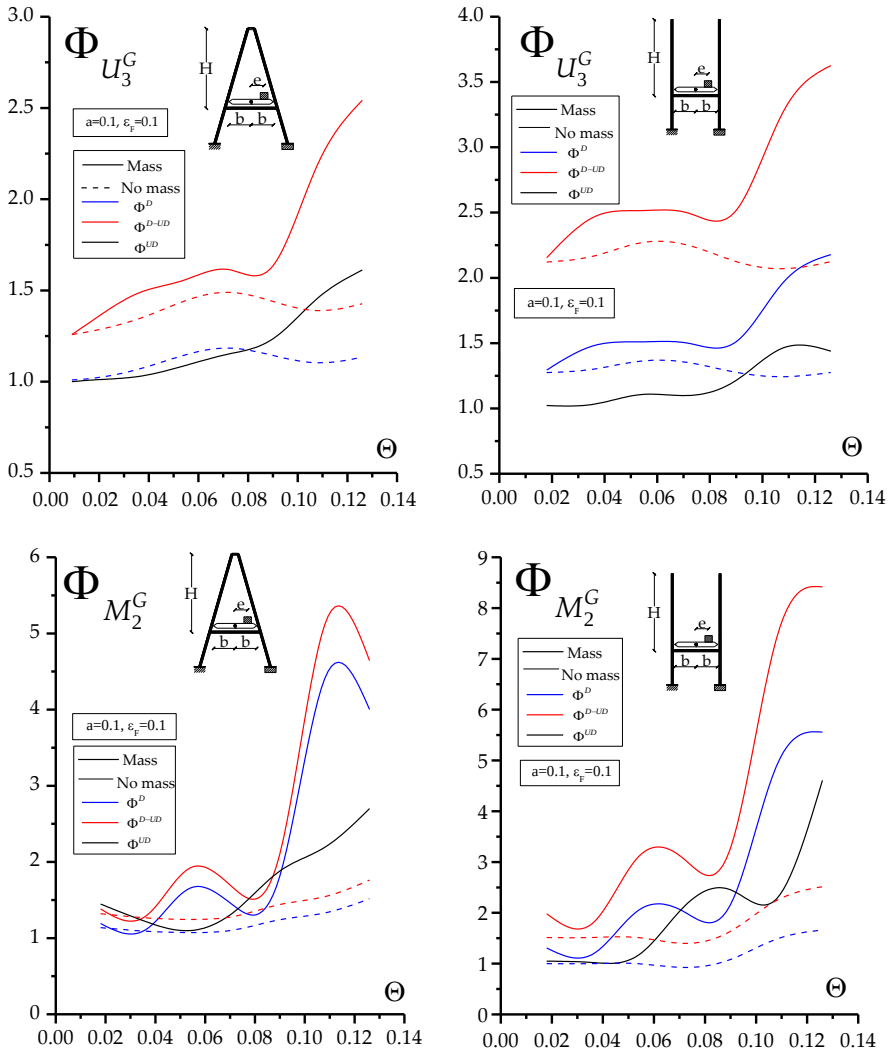

Figure 10. Dynamic amplification factors of the midspan vertical displacement for a bridge structure with H-shaped tower as a function of the normalized speed parameter: effect of the failure mechanism and moving load schematization

As a matter of fact, the ranges of maximum value of the DAFs increase from [1.47-1.52] in the undamaged configuration to [2.5-3.6] in the damaged one for the midspan displacement, and similarly from [2.5-4.5] to [5.4-8.3] for the midspan bending moment. It is worth noting that the DAFs from the undamaged bridge configuration are affected by large amplifications, especially for the variables concerning the bending moments. This behavior can be explained in view of the prevailing truss behavior of the structure and the nonstandard

inertial forces arising from the moving load application, which produce larger bending moments with respect to the ones obtained in the static configuration [8]. For all investigated cases, the bridge structures based on *H*-shaped tower topology are affected by larger dynamic amplifications than those observed in the structures based on *A*-shaped tower. This behavior can be explained in view of the differences in the cable stress distribution between undamaged and damages structures. In particular, the H-shaped tower bridges with respect to the *A*-shaped ones, owing to the failure of the lateral anchor stay, are affected by an unbalanced distribution of the internal stresses in the cable system, which produce larger torsional rotations and vertical displacements of the tower and the girder, respectively.

5 CONCLUSIONS

Long-span bridges under moving loads have been analyzed by means of tridimensional deformation modes, in terms of dynamic impact factors and maximum values of typical design bridge variables. The proposed model takes into account of nonlinearities involved by large displacements effects, whereas in those stays affected by internal damage, time dependent damage functions are introduced in the constitutive relationships. The purpose of this investigation is to analyze the amplification effects of the bridge structure produced by the moving load application and damage mechanisms in the cable system. The results have been analyzed with respect to several descriptions of the DAFs, which quantity the increments in the design bridge variables, i.e. bending moments and displacements, with respect to the static solution. The results denote that underestimations on the prediction of maximum values of both stresses and displacements are observed, if a transient analysis with a refined description of the inertial contributions is not carried out. The worst damage scenario that affects the cable-stayed bridges is the one associated with the failure of the anchor stay, which produces, also in the case of dead loading, displacements of the girder, DAFs and displacements much larger than the corresponding ones commonly recommended by the design prescriptions.

REFERENCES

[1] Post-Tensioning Institute (PTI). Recommendations for Stay Cable Design: Testing and Installation. Phoenix, Arizona, USA. 2007.

[2] Service d'Etudes Techniques des Routes et Autoroutes (SETRA). Haubans—Recommandations de la Commission Interministerielle de la Precontrainte. Bagneux F. 2001.

[3] Starossek , Haberland M. Approaches to measures of structural robustness. Struct Infrastruct E. 2011;7(7-8):625-31.

[4] Wolff M, Starossek U. Cable-loss analyses and collapse behavior of cable-stayed bridges. Bridge Maintenance, Safety, Management and Life-Cycle Optimization. 2010:2179-86.

[5] Zhou YF, Chen SR. Framework of Nonlinear Dynamic Simulation of Long-Span Cable-Stayed Bridge and Traffic System Subjected to Cable-Loss Incidents. J Struct Eng.

2016;142(3).
[6] Zhu J, Ye GR, Xiang YQ, Chen WQ. Dynamic behavior of cable-stayed beam with localized damage. J Vib Control. 2011;17(7):1080-9.
[7] Michaltsos GT, Raftoyiannis IG. The influence of a train's critical speed and rail discontinuity on the dynamic behavior of single-span steel bridges. Eng Struct. 2010;32(2):570-9.
[8] Bruno D, Greco F, Lonetti P. Dynamic impact analysis of long span cable-stayed bridges under moving loads. Eng Struct. 2008;30(4):1160-77.
[9] Gattulli V, Lepidi M. Localization and veering in the dynamics of cable-stayed bridges. Computers & Structures. 2007;85(21-22):1661-78.
[10] Faravelli L, Ubertini F. Nonlinear State Observation for Cable Dynamics. J Vib Control. 2009;15(7):1049-77.
[11] Greco F, Lonetti P, Pascuzzo A. Dynamic Analysis of Cable-Stayed Bridges Affected by Accidental Failure Mechanisms under Moving Loads. Mathematical Problems in Engineering. 2013.
[12] Lonetti P, Pascuzzo A. Vulnerability and failure analysis of hybrid cable-stayed suspension bridges subjected to damage mechanisms. Engineering Failure Analysis. 2014;45:470-95.
[13] Greco F, Leonetti L, Lonetti P. A novel approach based on ALE and delamination fracture mechanics for multilayered composite beams. Compos Part B-Eng. 2015;78:447-58.
[14] Barbero EJ, Lonetti P. Damage model for composites defined in terms of available data. Mech Compos Mater St. 2001;8(4):299-315.
[15] Mozos CM, Aparicio AC. Numerical and experimental study on the interaction cable structure during the failure of a stay in a cable stayed bridge. Eng Struct. 2011;33(8):2330-41.
[16] Fryba L. Vibration of solids and structures under moving loads. Telford T, editor. London (UK)1999.
[17] Lonetti P, Pascuzzo A. Optimum design analysis of hybrid cable-stayed suspension bridges. Advances in Engineering Software. 2014;73:53-66.
[18] Lonetti P, Pascuzzo A. Design analysis of the optimum configuration of self-anchored cable-stayed suspension bridges. Structural Engineering and Mechanics. 2014;51(5):847-66.
[19] Bruno D, Lonetti, P. and Pascuzzo, R. . An optimization model for the design of network arch bridges. Computer & Structures. 2016;170(1):13-25.
[20] Comsol. Reference Manual. Stockholm: Comsol. 2012.
[21] Bruno D, Greco, F.; Lonetti, P. A parametric study on the dynamic behavior of combined cable-stayed and suspension bridges under moving loads. International Journal of Computational Methods in Engineering Science and Mechanics. 2009;10(4):243-58.